A Carbon Nanotube-Based Hundred Watt-Level *Ka*-Band Backward Wave Oscillator

Xuesong Yuan, Qingyun Chen, Xiaotao Xu, Matthew T. Cole, *Senior Member, IEEE*, Yu Zhang, Zexiang Chen, and Yang Yan

***Abstract*— Carbon nanotube (CNT) cold-cathodes hold much promise in a variety of millimeter-wave and terahertz vacuum electronic radiation devices due to their inherent near instantaneous temporal turn-on and near-ideal ideal field electron emission performance. Here we report on the development of a CNT cold-cathode *Ka*-band backward-wave oscillator (BWO). Using a novel beam compression stage, theoretical studies, simulation results, and empirical findings collectively demonstrate that this device affords an unprecedentedly high output power of 230 W at a technologically important operating frequency of 33.65 GHz. The developed magnetic injection electron gun achieves a high emission current of 265.5 mA (emission current density of 188.3 mA/cm^2) and a high focused beam current density of 18.5 A/cm^2, which our studies suggest, is essential to the BWOs high output power.**

***Index Terms*— Backward wave oscillator (BWO), carbon nanotube (CNT), cold cathode, field emission (FE), high power, millimeter-wave (MMW) radiation.**

I. Introduction

OWING to their high output power and high operating frequency, vacuum electronic radiation sources (VERS) have been deployed widely in many technologies, including radar, biology, imaging, and communications [1]–[4]. At present, commercially available VERS typically utilize conventional thermionic cathode electron guns that are bulky and require additional heater driver electronics. Thermionic sources are inherently functionally limited due to their high-temperature operation and comparatively slow temporal response [5], [6]. Electron emission from thermionic cathodes requires comparatively lengthy preheating and thermalization times, which are often tens to hundreds of seconds. Though not particularly problematic during operation, the removal of additional heating circuitry from the electron sources helps drive important mass and volume reduction—a system-level design priority in many VERS applications. Perhaps the most pressing challenge facing thermionic-based devices is the ongoing difficulty in source miniaturization. As a result, research on the development of millimeter-wave (MMW) VERS has been largely stifled due to the lack of suitable emission sources which to develop new VERS on.

Though much-hyped, functional assessment of field emission (FE) cold cathode material continues to highlight them as the leading alternative for the replacement of incumbent thermionic electron sources in MMW VERS [7], [8]. Nanostructured cold cathodes have come to the fore in the vacuum electronics community due to their engineered surface properties and nanoscale morphologies, which allow for room temperature operation [9], self-ballasting emission [10], low turn-on voltages [11], and time stable electron emission [12]–[14]. The near-instantaneous switch-ON time [15] of such nanostructured FE sources removes the need for any preheating or thermal conditioning of the electron emitter. Nanostructured FE sources have long lifetimes [14], and facile system architectures [16], [17] are inexpensive to integrate due to their design simplicity, all of which allow for aggressive volume and mass miniaturization [17]–[22]. Within the absence of surface-bound adsorbents, carbon nanotubes (CNTs) emitters afford significantly extended operation times compared to other electron source technologies [14]. Though the emergence of a wide variety of new 1-D and 2-D materials has stimulated a revival in electron emission-based research, due to their comparative maturity CNTs remain one of the most attractive materials upon which to develop electron emission devices [23]. Their high electronic and thermal conductivity, large aspect ratio, and excellent chemical and mechanical stability continue to drive significant on-going research efforts [23]–[26]. To date, several attempts have been made to increase the FE current from CNT cold-cathodes and integrate them into VERS devices to support the development of new technologies [21], [24], [26]. Previously, we have designed a truncated-cone CNT cold-cathode electron gun

Manuscript received January 21, 2021; revised March 3, 2021; accepted March 10, 2021. This work was supported in part by the National Key Research and Development Program of China under Grant 2019YFA0210202, in part by the National Natural Science Foundation of China under Grant 61771096, in part by the Sichuan Science and Technology Program under Grant 2021YJ0096, and in part by the Fundamental Research Funds for the Central Universities under Grant ZYGX2019J012. The review of this article was arranged by Editor R. Letizia. *(Xuesong Yuan and Qingyun Chen are co-first authors.) (Corresponding author: Xuesong Yuan.)*

Xuesong Yuan, Qingyun Chen, Xiaotao Xu, and Yang Yan are with the School of Electronic Science and Engineering, University of Electronic Science and Technology of China, Chengdu 610054, China (e-mail: yuanxs@uestc.edu.cn; cqy@uestc.edu.cn).

Matthew T. Cole is with the Department of Electronic and Electrical Engineering, University of Bath, Bath BA2 7AY, U.K. (e-mail: m.t.cole@bath.ac.uk).

Yu Zhang is with the State Key Laboratory Optoelectronic Materials and Technologies, Sun Yat-sen University, Guangzhou 510275, China (e-mail: stszhyu@mail.sysu.edu.cn).

Zexiang Chen is with the School of Optoelectronic Science and Engineering, University of Electronic Science and Technology of China, Chengdu 610054, China (e-mail: zxchen@uestc.edu.cn).

Color versions of one or more figures in this article are available at https://doi.org/10.1109/TED.2021.3066144.

Digital Object Identifier 10.1109/TED.2021.3066144

with beam transmission of nearly 100% and a maximum emission current of 100 mA [16]. This electron gun was successfully used to develop a fully sealed 0.22-THz-gyrotron with an output power of 500 mW [27]. These systems demonstrate viable integration pathways toward the development of a new generation of functionally advanced nanomaterial-based cold-cathode VERS. Nevertheless, the output power of this gyrotron remained limited to only a few hundred milliwatts, making it unsuitable for many applications which require orders of magnitude higher output powers [26]. This work was extended by Li *et al.* [28] who used our truncated-cone CNT cold-cathode as a reference device when they developed a magnetic-focused X-band traveling wave tube (TWT) capable of delivering an emission current of 358 μA at 12.5 kV/mm. Unfortunately, the CNT cathode was damaged during pulsed mode testing, and the output power of their TWT was not extensively characterized or reported [28]. To date, principally due to the comparatively low emission current density achieved, there has been very little progress in producing high power MMW and terahertz VERS based on CNT cold cathode that is capable of operating at hundreds of watts [29]–[33]. This report looks to address this.

Capable of generating microwaves up to the THz frequency range, one of the most established VERS devices is the backward-wave oscillator (BWO). The emission frequency of BWOs is largely independent of the load impedance. As a result, BWOs can be designed to operate with exceptionally stable emission frequencies, enabling the realization of many previously unmanufacturable technologies [34]–[38]. In this article, we report on the development of a hundred watt-level BWO based on a CNT cold-cathode. On the basis of our earlier truncated-cone electron gun structure [16], we have optimized the cathode nanomaterial through precise control over the CNT growth to further improve emission current density to functionally useful levels. An operating current density of tens of A/cm^2 has been repeatedly achieved using a custom-designed high-compression-ratio electron gun design. Here, we report on the development of a proof-of-principle *Ka*-band disk-loaded waveguide BWO employing the improved CNT cold-cathode electron gun that delivers empirically tested output power of hundreds of watts. A hundred watt-level CNT cold-cathode VERS has been successfully realized, which lays important prototyping foundations for the development of future high-power terahertz VERS based on emerging nanomaterials.

II. Results

A. High-Performance CNT Cold-Cathode FE Characteristics

FE measurements were conducted using as-synthesized CNT-coated stainless steel (SS304) cathodes (see Section IV), with a control anode–cathode of 1.1 mm. The control anode is responsible for the electron extraction from the CNT emitters. The sidewalls of truncated-cone acted as the cold cathode substrate and the CNT forest has been directly synthesized on the whole substrate. The total emission area of the CNT cold cathode was estimated to be $1.41(\pm 0.01)$ cm^2. Typical current density–electric field (I–E) characteristics from the CNT cold

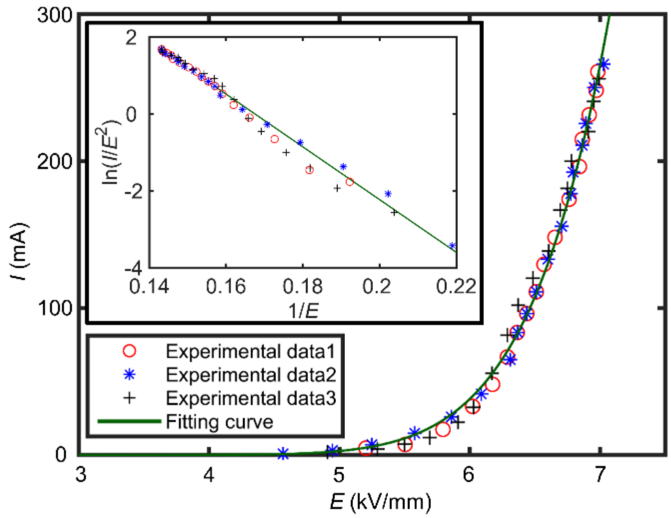

Fig. 1. Experimental results of the current (I)–electric field (E) characteristic of the truncated-cone CNT cold-cathode: emission current as a function of applied electric field, inset: FN plot.

cathodes are shown in Fig. 1. Measured from $n = 5$ samples, we observe a typical maximum emission current of 265.5 mA (emission current density of 188.3 mA/cm^2) for an applied electric field of 7 kV/mm, and there are few differences in FE characteristic of all samples. Used for simplicity the emission is broadly described by the simplified Fowler–Nordheim (FN) equation: $J = AE^2\exp(-B/E)$, where A and B are the FN constants. To support the development of our representative macroscale models, A and B here have been estimated by numerical fitting based on our experimental data. Applying a fitting procedure (described elsewhere [30]) across all samples, we find $A = 6.93 \times 10^{-7}$ A/V^2 and $B = 6.86 \times 10^7$ V/m ($R^2 = 0.9872$ (red data), $R^2 = 0.9897$ (blue data), $R^2 = 0.9863$ (black data)). From this, a representative emission characteristic curve was obtained which has been used in subsequent emitter modeling. The threshold electric field was 4.7 kV/mm for an emission current of 1 mA.

B. High-Performance CNT Cold-Cathode FE Characteristics

The CNT cold-cathode BWO device consists of a magnetic injection CNT cold-cathode electron gun, disk-loaded waveguide slow-wave structure, collector, and output window. Fig. 2 shows, a cross-sectional schematic of the structure and an optical photograph of the manufactured device. A double anode electro-optical system is used. The output system is formed from a mode converter, as shown in Fig. 2(c). During operation, electrons are extracted from the CNT cold-cathode under the action of the applied electric field between the control anode and cathode. Owing to the influence of the local magnetic field ($B_z = 0.4$ T) in the cathode region [16], electrons adopt a cyclotron motion. These electrons are accelerated by the anode into the beam tunnel (i). During this migration, the electron beam has a nonzero longitudinal velocity and transverse velocity component. The ratio of the transverse-to-longitudinal velocity of the electron beam is 0.54. After the electron beam is compressed within the beam tunnel,

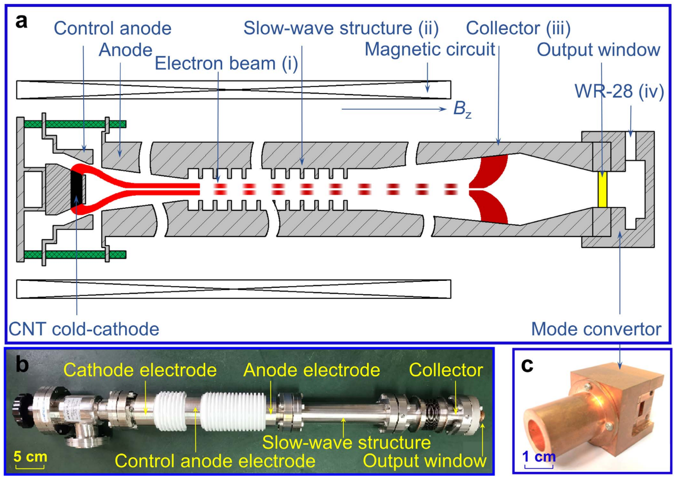

Fig. 2. (a) Cross-sectional illustration and (b) photograph of the CNT cold-cathode BWO (scale bar: 5 cm). (c) Photograph of the fabricated mode convertor (scale bar: 1 cm).

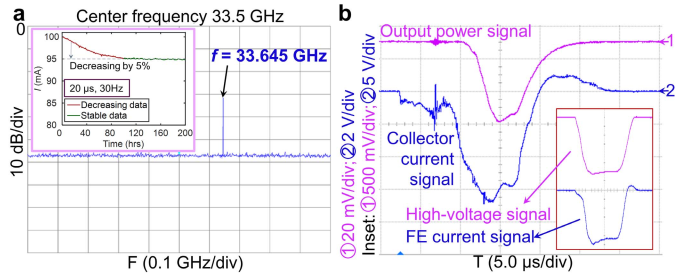

Fig. 3. Typical results of radiation output frequency and power measurement of the CNT cold-cathode BWO. (a) Peak spectra frequency of 33.645 GHz, inset: pulsed emission stability of CNT cold cathode. (b) Output power signal test results, inset: a typical temporal emission profile of the FE current and high-voltage signal in conventional diode mode measurements.

it enters the beam–wave interaction slow-wave structure (ii). The slow-wave structure consists of 15 disks loaded in the cylindrical waveguide with a waveguide inner diameter d_1 of 3.6 mm and a period length p of 2 mm. The thickness of disk t and the inner diameter of disk d_2 are 0.5 and 1.3 mm, respectively. Here, the electron beam interacts with the high frequency (HF) field (circular TM_{01} mode). The longitudinal energy of beams decreases, and the electromagnetic radiation of MMW is generated. Finally, the HF circular TM_{01} signal is output as a rectangular TE_{10} mode through the mode converter as the electron beam reaches the collector (iii). The output port (iv) of the circular waveguide TM_{01}-rectangular waveguide TE_{10} mode converter is WR-28 [39].

Experimentally, the CNT cold-cathode BWO was attached to an ultrahigh-vacuum system by a corrugated stainless-steel hose, with the entire evacuated system operating at a base pressure of 6.3×10^{-7} Pa. The CNT BWO measurements were performed using computer-controlled negative voltage pulses with a duration of 20 ($\pm$0.05) μs. The pulse repetition frequency was 30 ($\pm$0.1) Hz. A high-power matching load (attenuator) was connected to the output terminal of the CNT cold-cathode BWO through a directional coupler and mode converter. A low-power HF signal after attenuation was obtained using a directional coupler. The amplitude of the low-power HF signal was measured in triplicate using a *Ka*-band MMW detector (China Electronics Technology Instruments Company Ltd., Qingdao, China, AV70304). In addition, the frequency of the low-power HF signal was directly measured by a spectrum analyzer (China Electronics Technology Instruments Company Ltd., AV4036). When the negative voltage U_a of the cathode was increased from 36 to 38 kV, the output power signal was detected using a *Ka*-band MMW detector. The negative voltage U_g of the control anode was 28.8–30.4 kV based on the voltage division ratio of 4/5. Two operating frequencies of 33.412 and 33.645 GHz were measured using the spectrum analyzer. Typical results of the output frequency and measured power are given in Fig. 3. Fig. 3(a) shows the output frequency spectrum of the 33.645-GHz signal. Fig. 3(b) shows this peak's typical output power signal at an operation voltage of 37.4 kV. There is a delay between the peaks in the collector current and the output power associated with the MMW detector response of several microseconds due to measurements procedure used. Based on these findings, our calculations suggest that the output power of our BWO is approximately 230 W. The beam current is about 220 mA based on the collector current signal at an electric field of 6.9 kV/mm. According to the test profiles of our abovementioned FE measurements, the emission current is 224 mA at 6.9 kV/mm. The beam transmission is approximately 98.2%, which empirically aligns with the findings of our earlier work [16]. For an operation voltage of 36.8 kV, the measured output power was 220 W at a frequency of 33.412 GHz.

From the beam-compression-ratio of 100 reported in our earlier work, and the maximum emission current of 265.5 mA, coupled to a beam transmission of 98.2%, we estimate a beam current density in the HF tunnel to be approximately 18.5 A/cm^2. Such a high current density proves essential for the efficient operation of the MMW VERS. Owing to a large number of emitters per unit area of the emitter, which we estimate to be around $10^{8/}$cm^2, the emitted current per CNT emitter is, on average, low which ensures, time stable emission and addresses on-going functionality concerns within the nanomaterial-based FE community [21], [24], [40], [28]. Our data suggest that our CNT cathode has an emission current density of around the level of hundred mA/cm^2. The high final operating beam current density is attributed to the systems' subsequent high-compression-ratio, which creates the approximate three-orders of magnitude higher operating current density recorded and offers a viable technological solution to increasing the current density from CNT cold cathode in vacuum electron devices.

After 14 days of pulse-mode testing, the device showed a pulsed operating (20 μs, 30 Hz) lifetime of more than 100 h, with the FE current (100 mA) decreasing by only 5% throughout this entire duration as shown in the inset of Fig. 3(a). After the pulse-mode processing, the FE current has begun to level out dramatically with a stable current of ~95 mA during the testing time of 100 h. The operational magnetic field in the cathode region was only 0.4 T, supporting further system miniaturization. Should the cold cathodes engineered nanostructure be further optimized to achieve greater emission

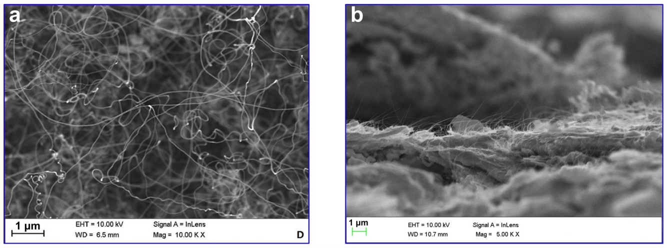

Fig. 4. Typical (a) areal-view SEM of an unoptimized misaligned and overly dense CNT cold cathode source [16] and (b) edge-view SEM of density and alignment optimized as-grown CNT thin film on a stainless steel substrate dense CNT forest, consisting of CNTs with mean diameter of 10 nm and mean length of 5 μm, as measured elsewhere [27], [32].

current densities, we believe, based on these findings, that such electron guns will ultimately replace incumbent hot cathodes in a wide range of applications and in doing so will provide a new vehicle for the development of the next generation of high power VERS devices.

III. Discussion

A. CNT Growth Optimization and CNT Cold-Cathode Modeling

In our previous research on the development of a 220-GHz cold-cathode gyrotron, high-density CNTs forests were used as the primary electron source [27]. In this earlier work, we successfully designed an electron-gun based on curved stainless steel (SS304) supported CNT cold-cathodes [16]. The final emission current was relatively low, only 28.2 mA, which was attributed to common electrostatic shielding effects resulting from the chemical vapor deposition (CVD) synthesized high-packing density CNTs (dense forests) [16], as shown in Fig. 4(a). As suggested elsewhere [33], in the present design, to mitigate this issue, a CNTs forest with lower relative density was employed to reduce electric field shielding effects, as shown in Fig. 4(b). Though vertically aligned CNTs have been shown to afford improved FE performance over their mis-orientated counterparts [33], CNT growth technology on curved substrates, such as those used here, remains challenging. Here we build on these preliminary designs, with a focus on their integration in a BWO. Efforts focused on improving the emission characteristics of the nanostructured cathode substrate material and engineering the CNT growth and subsequent geometry to increase their maximum emission current. Initial growth experiments resulted in the production of highly dense and misaligned CNTs. These emitters, though functional, demonstrated poor emission performance with unsatisfactory time stability. Upon optimization of the CNT growth (see Section IV), to be reported elsewhere [32], we reduced the CNT packing density and increased the typical vertical alignment of the CNTs on the emitter. These two morphological effects resulted in dramatically reduced nearest neighbor electrostatic shielding between CNTs as well as increasing local electric field enhancement by increasing the mean aspect ratio across the emitter. Moreover, we found that under the high electric fields used, anisotropic torque induction in the CNTs caused by the tip growth adopted by the CNTs and the presence of the Fe catalyst nanoparticles within the CNT tips ensured that the CNTs aligned to, and stayed aligned with the electric field direction during BWO operation [27], [32].

B. Simulation of a Ka-Band Disk-Loaded Waveguide BWO

To analyze the experimental results, commercially available 3-D simulation software was used. Summarized simulations showing the transmission characteristic, dispersion, output power, and operating frequency are illustrated in Fig. 5. As there are 14 cavities in the HF circuit (15 disks loaded in the waveguide), 14 resonant frequencies have been obtained by calculating the S_{21}, as shown in Fig. 5(a). Our simulations confirm the formation of two resonant frequencies at 33.482 and 33.623 GHz among all of the resonant frequencies produced. Fig. 5(b) shows the dispersion curve of the TM_{01} mode as a function of the normalized wavenumber. The operating voltage of the gyrating electron beam is obtained by the relativistic velocity correction formula [41]. When operated at 37.4 kV, and the ratio of the longitudinal velocity and transverse velocity of the electron beam is 0.54, the beamline (longitudinal velocity line) is superimposed onto the dispersion curve, intercepting the dispersion curve at a frequency of 33.623 GHz. When the beam voltage decreases to 36.8 kV, the operating frequency is 33.482 GHz. These findings indicate that the operating voltage fluctuates around 37 kV. Fig. 5(c) shows simulation results of the instantaneous output power at an operating voltage of 37.4 kV. The average output power is uncommonly large, at around 300 W (half of the instantaneous output power). Fig. 5(d) shows the frequency spectrum of the electric field (in dB) in the output waveguide; the primary frequency mode is at 33.618 GHz, closely matching (by 99.92%) the operating frequencies in our experiments. When the operating voltage was set to 36.8 kV, the average output power is 290 W at an output frequency of 33.484 GHz, further corroborating our empirical findings.

IV. Materials and Methods

Multiwalled carbon nanotubes (MWCNTs) were grown on the sidewalls of an SS304 stainless steel truncated-cone by microwave plasma CVD. The SS304 substrate was coated with Al (10 nm) and Fe (1 nm) by thermal evaporation (Edwards E306). To synthesis the CNTs, catalyst samples were placed in a 2.45-GHz microwave plasma CVD system (ASTeX). The microwave power level was set to 1 kW, the reactor pressure to 2500 Pa and a gas flow of 180 sccm of H_2 and 20 sccm of CH_4. The growth temperature was 600 °C. A typical as-grown MWCNT sample is shown in Fig. 4(b).

In the CNT cold-cathode characteristic electron emission measurements, diode experiments were performed using negative voltage pulses. The cathode was connected to the negative high voltage and the control anode was connected to the earth through a protection resistor R_{p} (12.8 kΩ) and test resistor R_{test} (27 Ω). The beam currents I were acquired by measuring the voltage (U_{test}) across R_{test} using an oscilloscope (Hewlett Packard, 54845A). The voltage difference U_{c} between the cathode and the control anode was inferred by: $U_{\mathrm{c}} = U_0 - I(R_{\mathrm{p}} + R_{\mathrm{test}})$, here U_0 was the power supply output voltage.

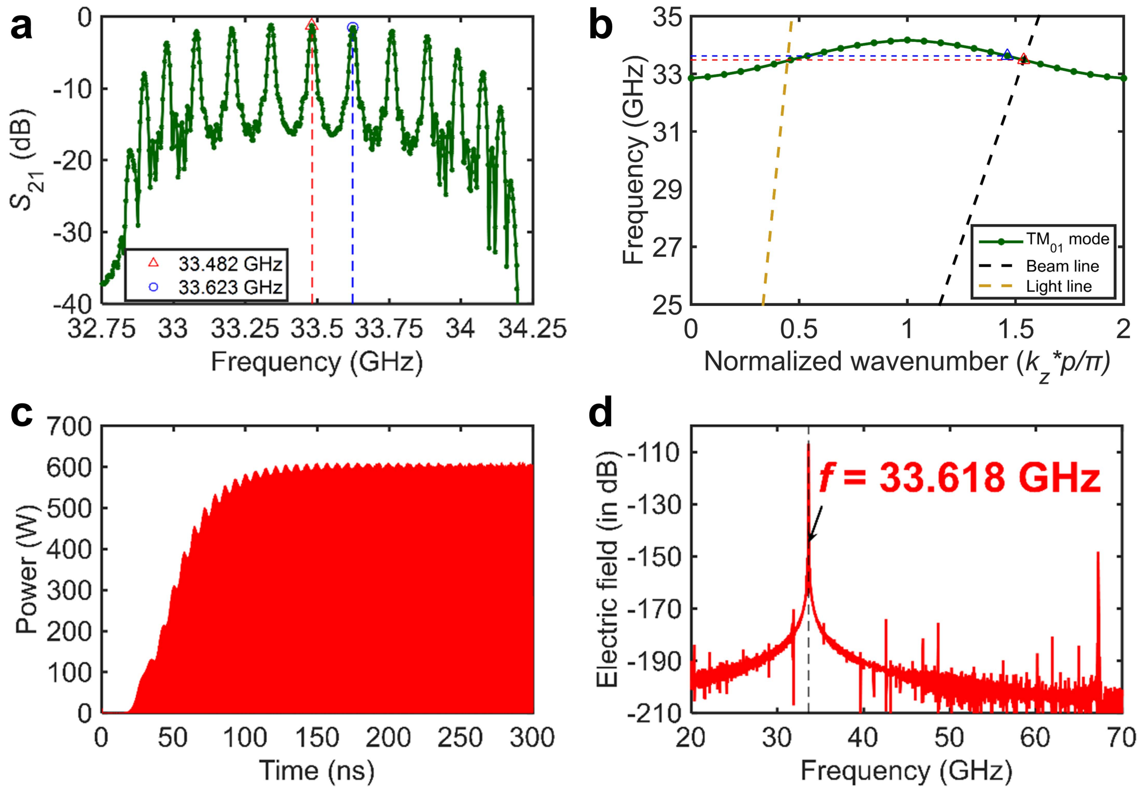

Fig. 5. Simulated results of the CNT cold-cathode BWO. (a) S_{21} transmission characteristic. (b) TM_{01} mode dispersion curve as a function of normalized wavenumber. (c) Output power signal showing a mean output power of 300 W. (d) Operating frequency of 33.618 GHz.

BWO device measurements were conducted using repeat pulsed mode operation with a typical pulse duration of 20 μs and a repetition frequency of 30 Hz. A negative high voltage power supply was applied to test the output signal. The applied high voltage was divided by resistances R_1 and R_2 to provide a negative high voltage for the CNT cold cathode and control anode. The ratio of R_1 and R_2 was dynamically adjusted according to the experimental requirements. The HF system and collector were connected to the earth through R_{test}. An oscilloscope (Hewlett Packard, 54845A) was used to detect both the high voltage signal by the resistor R_{test} and the output power signal amplitude of CNT cold-cathode BWO through the MMW detector. Because the pulse output power of the device was much higher than the average power, it was difficult to directly measure using the power meter. During the test, the output power signal of the BWO was connected first to the matching load through a directional coupler. The MMW detector was then connected to the directional coupler through an attenuator. For example, detector output power signal amplitude is shown in Fig. 3(b). The attenuation associated with the attenuator and mode converter was measured using a vector network analyzer (China Electronics Technology Instruments Company Ltd., AV3672C). There was a measured −73-dB attenuation from the output port of BWO to the input port of the detector. Finally, the same frequency MMW signal was fed into the detector using a standard signal source (China Electronics Technology Instruments Company Ltd., AV1464B) to obtain the same waveform amplitude. The actual output power of our BWO was measured by recording the output power of the standard signal source and dividing it by the linear value (5×10^{-8}) of −73-dB attenuation extracted from our measurement setup. The operating frequency was directly obtained by the spectrum analyzer through waveguide coaxial conversion.

V. Conclusion

Here, we demonstrate a hundred watt-level *Ka*-band BWO using a CNT-based field electron emitter. By capitalizing on recent developments in the CNT manufacturing technology and advances in materials science, we have demonstrated a viable route to achieve emission beam currents of up to 265.5 mA (emission current density of 188.3 mA/cm^2). Stable focused beam current densities of 18.5 A/cm^2 have been demonstrated, validating our previous experimental results. Here output powers a factor of 10^3 larger than the present state-of-the-art mW levels have been achieved, which represents a significant breakthrough in the use of nanostructured cold-cathodes in advancing the state-of-the-art in VERS design, fabrication, and operation.

References

[1] R. J. Barker and E. Schamiloglu, "Introduction," in *High-Power Microwave Sources and Technologies*, R. J. Barker and E. Schamiloglu, Eds. Piscataway, NJ, USA: IEEE Press, 2001, ch. 1, pp. 1–6.

[2] J. H. Booske *et al.*, "Vacuum electronic high power terahertz sources," *IEEE Trans. THz Sci. Technol.*, vol. 1, no. 1, pp. 54–75, Sep. 2011, doi: 10.1109/Tthz.2011.2151610.

[3] J. H. Booske, "Plasma physics and related challenges of millimeter-wave-to-terahertz and high power microwave generation," *Phys. Plasmas*, vol. 15, no. 5, May 2008, Art. no. 055502, doi: 10.1063/1.2838240.

[4] A. A. Borisov *et al.*, "The development of vacuum microwave devices in Istok," in *Proc. IEEE Int. Vac. Electron. Conf. (IVEC)*, Bengaluru, India, Feb. 2011, pp. 437–438.

[5] J. Pasour *et al.*, "Demonstration of a 100-kW solenoidally focused sheet electron beam for millimeter-wave amplifiers," *IEEE Trans. Electron Devices*, vol. 58, no. 6, pp. 1792–1797, Jun. 2011, doi: 10.1109/Ted.2011.2126577.

[6] R. Li, C. Ruan, A. K. Fahad, C. Zhang, and S. Li, "Broadband and high-power terahertz radiation source based on extended interaction klystron," *Sci. Rep.*, vol. 9, no. 1, p. 4584, Mar. 2019, doi: 10.1038/s41598-019-41087-3.

[7] D. R. Whaley, R. Duggal, C. M. Armstrong, C. L. Bellew, C. E. Holland, and C. A. Spindt, "100 W operation of a cold cathode TWT," *IEEE Trans. Electron Devices*, vol. 56, no. 5, pp. 896–905, May 2009.

[8] M. Garven, S. N. Spark, A. W. Cross, S. J. Cooke, and A. D. R. Phelps, "Gyrotron experiments employing a field emission array cathode," *Phys. Rev. Lett.*, vol. 77, no. 11, pp. 2320–2323, Sep. 1996, doi: 10.1103/physrevlett.77.2320.

[9] S. Berhanu *et al.*, "Microscopic analysis of performance variations in carbon nanotube field emission cathodes: Implications for device optimization," *Phys. Status Solidi (A)*, vol. 209, no. 11, pp. 2114–2125, Nov. 2012, doi: 10.1002/pssa.201228296.

[10] C. Li *et al.*, "Stable, self-ballasting field emission from zinc oxide nanowires grown on an array of vertically aligned carbon nanofibers," *Appl. Phys. Lett.*, vol. 96, no. 14, Apr. 2010, Art. no. 143114, doi: 10.1063/1.3380597.

[11] K. B. K. Teo *et al.*, "Microwave devices: Carbon nanotubes as cold cathodes," *Nature*, vol. 437, no. 7061, p. 968, 2005, doi: 10.1038/437968a.

[12] L. T. Williams, V. S. Kumsomboone, W. J. Ready, and M. L. R. Walker, "Lifetime and failure mechanisms of an arrayed carbon nanotube field emission cathode," *IEEE Trans. Electron Devices*, vol. 57, no. 11, pp. 3163–3168, Nov. 2010, doi: 10.1109/TED.2010.2069563.

[13] A. M. Fennimore, D. H. Roach, G. A. Wilson, F. M. Pellicone, and L. T. Cheng, "Enhancing lifetime of carbon nanotube field emitters through hydrocarbon exposure," *Appl. Phys. Lett.*, vol. 92, no. 21, May 2008, Art. no. 213108, doi: 10.1063/1.2936960.

[14] N. S. Xu and S. E. Huq, "Novel cold cathode materials and applications," *Mater. Sci. Eng., R, Rep.*, vol. 48, no. 2, pp. 47–189, Jan. 2005, doi: 10.1016/j.mser.2004.12.001.

[15] C. Li *et al.*, "Carbon nanotubes: Carbon nanotubes as an ultrafast emitter with a narrow energy spread at optical frequency," *Adv. Mater.*, vol. 29, no. 30, Aug. 2017, Art. no. 1701580, doi: 10.1002/adma.201770216.

[16] X. Yuan *et al.*, "A truncated-cone carbon nanotube cold-cathode electron gun," *Carbon*, vol. 120, pp. 374–379, Aug. 2017, doi: 10.1016/j.carbon.2017.03.046.

[17] X. Yuan *et al.*, "A gridded high-compression-ratio carbon nanotube cold cathode electron gun," *IEEE Electron Device Lett.*, vol. 36, no. 4, pp. 399–401, Apr. 2015, doi: 10.1109/LED.2015.2401593.

[18] Y. Saito and S. Uemura, "Field emission from carbon nanotubes and its application to electron sources," *Carbon*, vol. 38, no. 2, pp. 169–182, 2000, doi: 10.1016/S0008-6223(99)00139-6.

[19] P. Liu, Y. Wei, K. Liu, L. Liu, K. Jiang, and S. Fan, "New-type planar field emission display with superaligned carbon nanotube yarn emitter," *Nano Lett.*, vol. 12, no. 5, pp. 2391–2396, May 2012, doi: 10.1021/nl3003792.

[20] J.-W. Jeong, J.-W. Kim, J.-T. Kang, S. Choi, S. Ahn, and Y.-H. Song, "A vacuum-sealed compact X-ray tube based on focused carbon nanotube field-emission electrons," *Nanotechnology*, vol. 24, no. 8, Mar. 2013, Art. no. 085201, doi: 10.1088/0957-4484/24/8/085201.

[21] H. J. Kim, J. J. Choi, J.-H. Han, J. H. Park, and J.-B. Yoo, "Design and field emission test of carbon nanotube pasted cathodes for traveling-wave tube applications," *IEEE Trans. Electron Devices*, vol. 53, no. 11, pp. 2674–2680, Nov. 2006, doi: 10.1109/TED.2006.884076.

[22] Q. Chen *et al.*, "Study on a high beam transparency gridded X-ray electron gun based on carbon nanotube cold cathode," *J. Nanoelectron. Optoelectron.*, vol. 13, no. 9, pp. 1265–1270, Sep. 2018, doi: 10.1166/jno.2018.2364.

[23] C. M. Collins, R. J. Parmee, W. I. Milne, and M. T. Cole, "High performance field emitters," *Adv. Sci.*, vol. 3, no. 5, May 2016, Art. no. 1500318, doi: 10.1002/advs.201500318.

[24] W. I. Milne and K. B. K. Teo, "Aligned carbon nanotubes/fibers for applications in vacuum microwave amplifiers," *J. Vac. Sci. Technol. B, Microelectron.*, vol. 24, no. 1, pp. 345–348, Jan./Feb. 2006, doi: 10.1116/1.2161223.

[25] G. Ulisse *et al.*, "Carbon nanotube cathodes for electron gun," *IEEE Electron Device Lett.*, vol. 34, no. 5, pp. 698–700, May 2013, doi: 10.1109/LED.2013.2250247.

[26] H. M. Manohara, R. Toda, R. H. Lin, A. Liao, M. J. Bronikowski, and P. H. Siegel, "Carbon nanotube bundle array cold cathodes for THz vacuum tube sources," *J. Infr., Millim., THz Waves*, vol. 30, no. 12, pp. 1338–1350, Jul. 2009, doi: 10.1007/s10762-009-9547-x.

[27] X. Yuan *et al.*, "A fully-sealed carbon-nanotube cold-cathode terahertz gyrotron," *Sci. Rep.*, vol. 6, no. 1, p. 32936, Dec. 2016, doi: 10.1038/srep32936.

[28] X. Li, B. Chen, Y. Feng, Y. Zhang, S. Deng, and J. Feng, "Beam test of a novel CNT cathode-based electron gun assembled in a TWT," *IEEE Trans. Electron Devices*, vol. 66, no. 5, pp. 2382–2388, May 2019, doi: 10.1109/TED.2019.2902385.

[29] X. Yuan, M. Cole, Y. Zhang, J. Wu, W. Milne, and Y. Yan, "Parametrically optimized carbon nanotube-coated cold cathode spindt arrays," *Nanomaterials*, vol. 7, no. 1, p. 13, Jan. 2017, doi: 10.3390/nano7010013.

[30] Y. Xue-Song *et al.*, "Study of pulsed field emission characteristics and simulation models of carbon nanotube cold cathodes," *Wuli Xuebao/Acta Phys. Sinica*, vol. 61, no. 21, 2012, Art. no. 216101.

[31] X. Yuan *et al.*, "Theoretical research on a multibeam-modulated electron gun based on carbon nanotube cold cathodes," *IEEE Trans. Electron Devices*, vol. 63, no. 7, pp. 2919–2924, Jul. 2016, doi: 10.1109/TED.2016.2565583.

[32] M. T. Cole *et al.*, "*In-situ* deposition of sparse vertically aligned carbon nanofibres on catalytically activated stainless steel mesh for field emission applications," *Diamond Rel. Mater.*, vol. 23, pp. 66–71, Mar. 2012, doi: 10.1016/j.diamond.2011.12.039.

[33] M. T. Cole, K. B. K. Teo, O. Gröening, L. Gangloff, P. Legagneux, and W. I. Milne, "Deterministic cold cathode electron emission from carbon nanofibre arrays," *Sci. Rep.*, vol. 4, no. 1, p. 4840, May 2015, doi: 10.1038/srep04840.

[34] M. I. Yalandin, S. N. Rukin, V. G. Shpak, S. A. Shunailov, V. V. Rostov, and G. A. Mesyats, "Highly effective, repetitive nanosecond-range Ka-band BWO," in *Proc. IEEE Int. Power Modulators High-Voltage Conf.*, May 2008, pp. 402–404.

[35] R. A. Kehs *et al.*, "A high-power backward-wave oscillator driven by a relativistic electron beam," *IEEE Trans. Plasma Sci.*, vol. PS-13, no. 6, pp. 559–562, Dec. 1985, doi: 10.1109/TPS.1985.4316473.

[36] Z. Wang *et al.*, "High-power millimeter-wave BWO driven by sheet electron beam," *IEEE Trans. Electron Devices*, vol. 60, no. 1, pp. 471–477, Jan. 2013, doi: 10.1109/Ted.2012.2226587.

[37] M. I. Yalandin *et al.*, "Compact Ka-band backward-wave generator of superradiative pulses operating at reduced guiding magnetic field," *IEEE Trans. Plasma Sci.*, vol. 36, no. 5, pp. 2604–2608, Oct. 2008, doi: 10.1109/Tps.2008.2004244.

[38] Q. Chen, X. Yuan, M. Cole, Y. Zhang, L. Meng, and Y. Yan, "Theoretical study of a 0.22 THz backward wave oscillator based on a dual-gridded, carbon-nanotube cold cathode," *Appl. Sci.*, vol. 8, no. 12, p. 2462, Dec. 2018.

[39] Q. Chen *et al.*, "Development of a Ka-band circular TM_{01} to rectangular TE_{10} mode converter," *IEEE Trans. Electron Devices*, vol. 67, no. 3, pp. 1254–1258, Mar. 2020, doi: 10.1109/TED.2020.2968347.

[40] W. A. de Heer, A. C. Telain, and D. Ugarte, "A carbon nanotube field-emission electron source," *Science*, vol. 270, no. 5239, pp. 1179–1180, Nov. 1995, doi: 10.1126/science.270.5239.1179.

[41] A. S. Gilmour and I. Ebrary, *Klystrons, Traveling Wave Tubes, Magnetrons, Crossed-Field Amplifiers, and Gyrotrons*. Fitchburg, MA, USA: Artech House, 2011, p. 21.